

P8B.11 REAL-TIME WIND FIELD RETRIEVAL SYSTEM BY USING X-BAND RADAR NETWORK AROUND TOKYO METROPOLITAN AREA

Takeshi Maesaka*, Masayuki Maki, Koyuru Iwanami, Ryohei Misumi, and Shingo Shimizu
National Research Institute for Earth Science and Disaster Prevention, Japan

1. INTRODUCTION

In recent years, it has been pointed out that urban area implies a vulnerability to severe weather. Since weather surveillance radar is a suitable tool to monitor it, universities and research institutes have installed the radars for studying disaster mitigations and cloud–precipitation process; however they are operated individually for individual purpose. Furthermore, most of those radar are X-band radars, which were regarded as an unsuitable radar for Quantitative Precipitation Estimate (QPE) because of the attenuation. In 2000, National Research Institute for Earth Science and Disaster Prevention (NIED), Japan, developed a X-band Multi-Parameter radar (hereafter referred to MP radar), which is a dual polarization radar to observe Z_h , V , W , Z_{DR} , ρ_{HV} , and $\Phi_{DP}(K_{DP})$. Maki *et al.* (2005a, b) and Park *et al.* (2005) showed the rainfall estimation using K_{DP} data measured by MP radar, which was more accurate than reflectivity based estimation.

Now we are developing X-band radar network (hereafter referred to X-NET), which consists of such individual radars around Tokyo metropolitan area (Fig. 1). The networking relieves an attenuation problem of X-band radar, and enables to estimate wind fields by using their Doppler velocity data. Especially, due to recent severe wind disasters in Japan, wind information near the ground surface is now needed for disaster mitigation and wind engineering. In this paper, we describe the real-time wind field retrieval system by using the X-band radar network and its applications to estimate the wind information near the ground surface.

2. X-NET

There are some advantages to construct the network of X-band radars. The observation range of X-band radar tends to be shorter than those of S-band or C-band radars. It enables to expand the observation area. Moreover, Undetectable area due to the attenuation is covered by one another. It is equally important to retrieve wind field by synthesizing Doppler velocities observed by the radars which belong to the network. X-NET is planned under the consideration of these

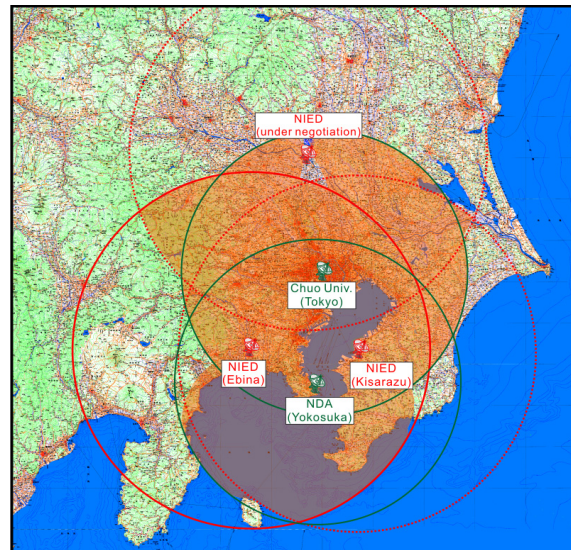


Figure 1: Radar distribution and observation area of X-NET (expected during the warm season in 2008). Three red radars indicate locations of NIED MP radars at Ebina, Kisarazu (under reconstruction, to be completed by January 2008), and north of metropolitan area (The installing location is under negotiation.). Two green radars indicate the locations of Doppler radars operated by Chuo University at Tokyo and National Defense Academy (NDA) at Yokosuka. Red and green circles indicate the observation areas of NIED MP radars ($r=80$ km) and Doppler radars ($r=64$ km). The area in which the wind speed and direction can be retrieved, is shown by red shadow.

* Corresponding author address: Takeshi Maesaka, National Research Institute for Earth Science and Disaster Prevention, 3-1 Tennodai, Tsukuba, Ibaraki, Japan, 305-0006. e-mail: maesaka@bosai.go.jp

advantages to detect the heavy rainfall and the severe wind disaster.

Figure 1 indicates the X-NET radar distribution and the observation area expected during the warm season in 2007. NIED plans to install three MP radars around the Tokyo metropolitan area. MP radar at Ebina was installed in 2003. As for the radar at Kisarazu, it is now under reconstruction, and will be installed by January 2008. Additionally, NIED has another MP radar, which is located at Snow and Ice Research Center of NIED at Nagaoka during the winter season, and plans to move it to the north of the metropolitan area during the warm season. The Doppler radars of Chuo University and National Defense Academy (NDA) also join the network to support the wind field retrieval, although these cannot acquire the polarimetric parameters. The radar network enables to estimate the wind field in the metropolitan and bay areas.

The observed radar data are immediately transported to NIED at Tsukuba via the Internet or a closed IP network. Then various products (wind speed and direction, rainfall intensity, rainfall nowcasting, landslide and urban flood risk informations, etc...) are generated from the radar data, and these are provided in real-time on the web site. Furthermore, the radar data are used for the data assimilation with cloud-resolving numerical model to make a short-term forecast of rainfall (Shimizu *et al.* 2007).

3. WIND FIELD RETRIEVAL SYSTEM

The radar data gathered in NIED at Tsukuba are then input to the wind field retrieval system, which consists of two parts: unaliasing and synthesis of Doppler velocities.

3.1 Unaliasing of Doppler velocity

A dual-PRF method is now available in recent radar system; however our X-band radar network includes the radar in which the dual-PRF method is not available. So the automated unaliasing is necessary prior to the wind synthesis. At first, we compare the velocity data with the output of

operational mesoscale model which is distributed by Japan Meteorological Agency every 3 hours. Then velocity data are unaliased by the assumptions of VAD, temporal continuity and spatial continuity step by step. This method were examined with the typhoon event in 2005, and showed the reliable performance.

3.2 Doppler velocity synthesis

The multiple Doppler velocity synthesis is based on a variational method (e.g. Bousquet and Chong 1998, Gao *et al.* 1999) which minimizes the cost function which is defined by a difference between observed and estimated velocities, mass continuity, and Laplacian of the estimated wind fields. To estimate the wind information near the ground surface, a logarithmic velocity profile is assumed below the bottom boundary of the data grid to which radar data are interpolated ($z_1=500$ m ASL). The profile is expressed as,

$$u(z) = \frac{u^*}{\kappa} \log \frac{z - z_h}{z_0}, \quad (1)$$

$$v(z) = \frac{v^*}{\kappa} \log \frac{z - z_h}{z_0}, \quad (2)$$

where $u(z)$ and $v(z)$ are wind speeds at the height of z (ASL), u^* and v^* are friction velocities, κ is von Karman constant, z_h is a terrain height ASL, and z_0 is a surface roughness length. This assumption enables to calculate mas fluxes below the bottom boundary as,

$$F_x = \int_{z_h}^{z_1} \rho(z) u(z) dz, \quad (3)$$

$$F_y = \int_{z_h}^{z_1} \rho(z) v(z) dz, \quad (4)$$

$$(5)$$

where ρ is an air density. So vertical velocity at the bottom boundary is estimated as,

$$w_1 = -\frac{1}{\rho_1} \left(\frac{\partial F_x}{\partial x} + \frac{\partial F_y}{\partial y} \right), \quad (6)$$

and it is used as a bottom boundary data in an iterative process of variational solution. This vertical velocity includes the effect of a divergence

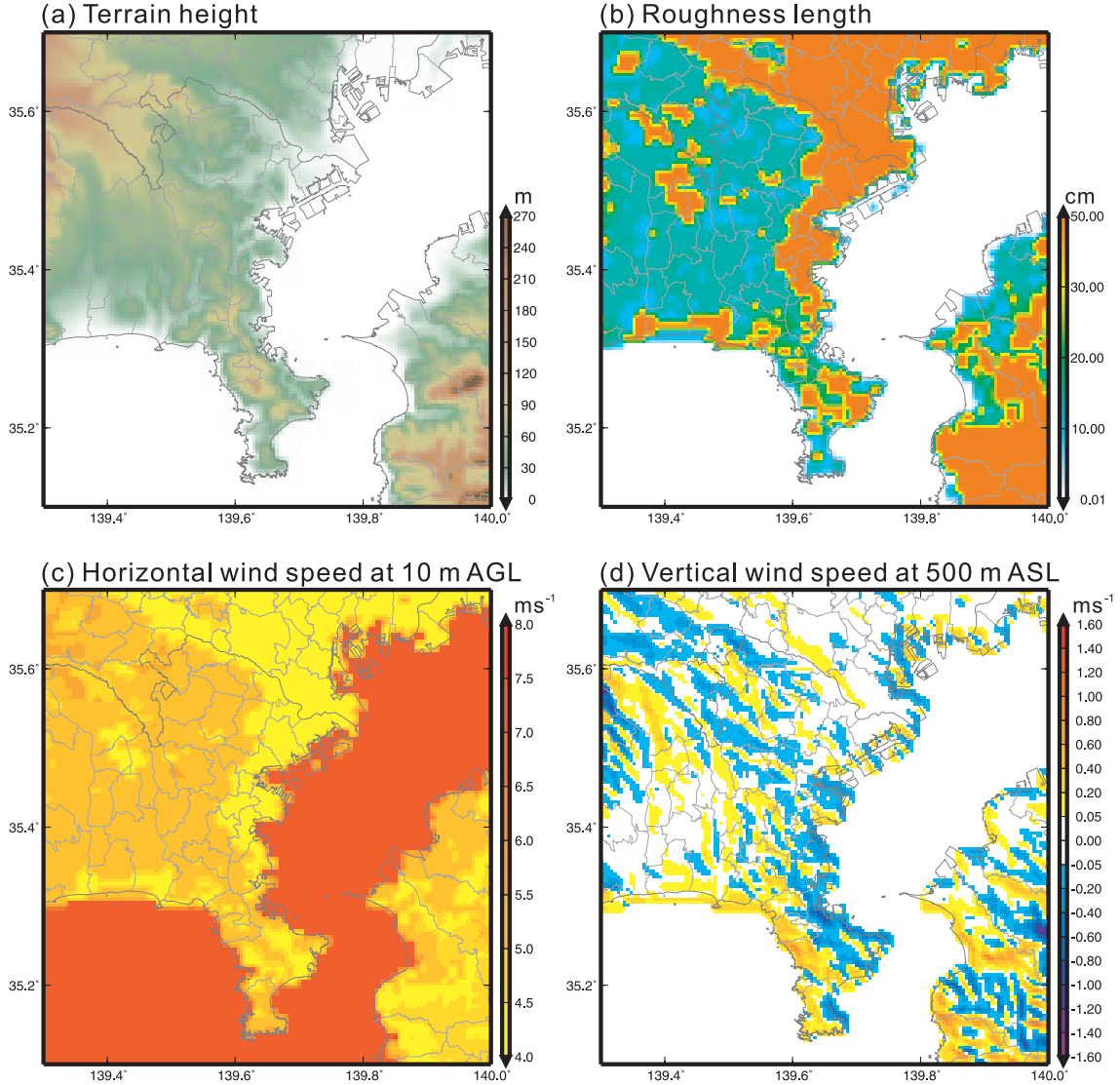


Figure 2: Responses of c) wind speed at the height of 10 m AGL and d) vertical velocity at the bottom boundary ($z=500$ m ASL) of the calculation grid, against the southwesterly of 10 ms^{-1} at the bottom boundary. a) Terrain height, and b) surface roughness length given in the wind retrieval system. Terrain height data are made by the interpolation of United States Geological Survey (USGS) GTOPO30 database. USGS land use database is also used to create surface roughness data.

caused by the difference of surface roughness, and impales the upward/downward motion by orographies.

Figure 2 indicates a responses of the wind speed near the ground surface ($z=10$ m AGL) and the vertical velocity at the bottom boundary of calculation grid, against the southwesterly flow of 10 ms^{-1} at the bottom boundary in the wind retrieval system. Horizontal wind speed near the ground surface (Fig. 2c) varies from 4.3 ms^{-1} to

7.5 ms^{-1} in accordance with the roughness distribution. Vertical wind speed at the height of 500 m ASL (Fig. 2d) represents the updraft (down-draft) by a frictional convergence (divergence) at the coastline, and also shows an orographic lifting.

Figure 3 indicates the wind field at 1230 JST¹ 15 July 2006, calculated by the wind retrieval system with radar observation data. At this time,

¹Japan Standard Time (JST=UTC+9).

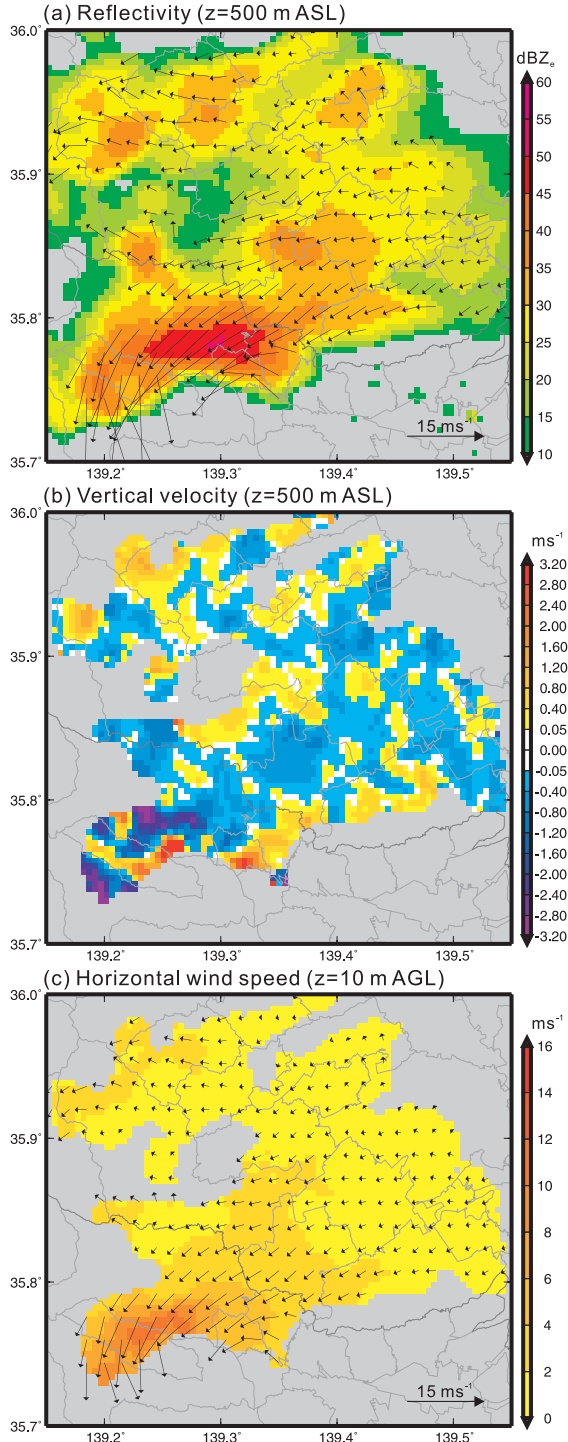


Figure 3: Wind fields at 1230 JST 15 July 2007. a) Reflectivity and horizontal wind (arrows), and b) vertical velocity at the bottom boundary of calculation grid (500 m ASL). c) Horizontal wind (arrows) and its speed near the ground surface (10 m AGL).

F0 wind damage was reported in the northwest part of Tokyo. The system analyzed a divergent flow with the wind speed over 10 ms⁻¹ near the ground surface (Fig. 3c).

4. CONCLUSION

X-band radar network is now developing around the Tokyo metropolitan area for the real-time monitoring of heavy rainfall and severe wind disaster. To estimate the wind information near the ground surface, the logarithmic velocity profile is assumed below the bottom boundary in the wind field retrieval system. The assumption enables to estimate not only wind speed near the ground surface but also vertical velocity at the bottom boundary, which considers with the surface roughness and orography. The performance of the retrieval system was examined with the radar observation data during the severe wind event, and it showed reasonable result. This wind field retrieval system is expected to provide a basic information for the mitigation of severe wind disaster.

Acknowledgment

We are grateful to Prof. Tadashi Yamada and Prof. Hirokazu Hirano (Chuo University, Japan) for providing Doppler radar data.

References

- Bousquet, O. and M. Chong, 1998: A multiple-Doppler synthesis and continuity adjustment technique (MUSCAT) to recover wind components from Doppler radar measurements. *J. atmos. oceanic technol.*, **15**, 343–359.
- Gao, J., M. Xue, A. Shapiro and K. K. Droege-meier, 1999: A variational method for the analysis of three-dimensional wind fields from two Doppler radars. *Mon. Wea. Rev.*, **127**, 2128–2142.
- Maki, M., K. Iwanami, R. Misumi, S.-G. Park, H. Moriwaki, K. Maruyama, I. Watabe, D.-I. Lee, M. Jang, H.-K. Kim, V.N. Bringi, and

- H. Uyeda, 2005a: Semi-operational rainfall observations with X-band multi-parameter radar, *Atmos. Sci. Letters*, **6**, 12–18.
- , S.-G. Park and V. N. Bringi, 2005b: Effect of natural variations in rain drop size distributions on rain rate estimators of 3 cm Wavelength polarimetric radar, *J. Meteor. Soc. Japan*, **83**, 871–893.
- , K. Iwanami, R. Misumi, T. Maesaka, S. Shimizu, K. Kieda, K. Nakane, A. Kato, K. Dairaku, H. Moriwaki, T. Fukuzono, S. Yazaki, Y. Sasaki, M. Tominaga and T. Nagasaka, 2006: Studies on the prediction of landslides and urban flooding using an X-band multi-parameter radar network, *Proc. Second Intn'l Symposium on Quantitative Precipitation Forecasting and Hydrology*, P3–8.
- Park, S.-G., M. Maki, K. Iwanami, V. N. Bringi, and V. Chandrasekar, 2005: Correction of radar reflectivity and differential reflectivity for rain attenuation at X-band wavelength. Part II: Evaluation and application. *J. Atmos. Oceanic Technol.*, **22**, 1633–1655.
- Shimizu, S., T. Maesaka, R. Misumi, K. Iwanami, M. Maki, T. Yamada, S. Tsutiya, and W. Sato, 2007: Development for a nudging assimilation procedure of cloud resolving storm simulator using multiparameter radar data. *Proc. of 33rd Conference on Radar Meteorology*, P4.7.